

A DATA ASSIMILATION STUDY FOR THE IDENTIFICATION OF SCALES GOVERNING GRID TURBULENCE DECAY

Vincent Mons, Jean-Camille Chassaing, Thomas Gomez
Institut Jean Le Rond d'Alembert
Sorbonne Univ, UPMC Univ Paris 06 and CNRS, UMR 7190
Paris, F-75005, France
vincent.mons@sfr.fr

Pierre Sagaut
Laboratoire de Mécanique, Modélisation et Procédés Propres
UMR CNRS 7340
Aix-Marseille Université
IMT La Jetée, Technopole de Château-Gombert
38, rue Frédéric Joliot-Curie
13451 Marseille Cedex 13, France
pierre.sagaut@uni-amu.fr

INTRODUCTION

The decay of incompressible homogeneous isotropic turbulence (HIT), which can be studied via grid turbulence experiments, is among the most important issue in turbulence theory, since isotropic turbulence is the framework in which the deepest investigations of nonlinear features of turbulence can be performed. Even though numerous studies have been devoted to HIT since about one century, many questions remain open. Among them, the identification of scales which govern the decay of HIT still deserves further investigations. Although there is consensus that the turbulent kinetic energy K , after a possible transient relaxation phase, follows an algebraic law, i.e. $K(t) \propto t^{n_K}$, the question of the dependence of the exponent n_K to some specific features of the initial condition has raised some controversies. However, the most recent works indicate that there is no universal regime and that the decay rate is definitely governed by the details of the initial condition. Indeed, it is generally stated in the literature that the exponent n_K is related to the asymptotic large-scale behavior of the longitudinal velocity correlation function $f(r, t = 0)$ in physical space, or equivalently, to the asymptotic behavior of the kinetic energy spectrum $E(k, t = 0)$ in spectral space. But it is worth keeping in mind that, due to technological limitations, the exact behavior of the velocity correlation function, or that of the energy spectrum, at scales much larger than the integral scale escapes both experimental and numerical investigation at the present time. Besides, the concept of large-scale asymptotic behavior is hard to reconcile with real-life turbulent flows, which are bounded in space and can be observed over finite times only. It is also interesting to note that the Comte-Bellot - Corrsin theory, which proves to be effective in predicting the value of the exponent n_K , relies on a single length scale which is the integral scale.

The aim of this study is to identify the scales which

govern the decay of HIT over finite time. Our approach involves the use of an optimal-control-based data assimilation technique; the methodology is the following. First, observations of a numerical reference decay are performed. Then, using these observations, an optimization procedure is employed to recover the initial condition of the reference decay, starting from an initial guess. The parts of the initial condition which are reconstructed by the optimization procedure are interpreted as having a significant impact on the decay. Besides, the optimization procedure also furnishes the gradient of the solution associated to the decay with respect to the initial condition, allowing a mathematically grounded identification of the scales which govern the decay. In order to investigate a wide range of initial conditions and flow regimes, it is chosen to use the Eddy-Damped Quasi-Normal Markovian (EDQNM) model to compute time evolution of the kinetic energy spectrum $E(k, t)$. This highly versatile model is known to yield very accurate results for isotropic turbulence decay with good resolution at both large and small scales, ensuring the reliability of the results. The adjoint EDQNM problem is derived in the present study for the purpose of the data assimilation procedure.

DATA ASSIMILATION METHOD FOR OPTIMAL RECONSTRUCTION OF THE INITIAL CONDITION

Given observations y of a reference EDQNM simulation, the nature of which will be specified later, the aim of the data assimilation technique is to minimize the discrepancies between y and a solution $E(k, t)$ of the EDQNM equations. This leads to the introduction of the Lagrangian

\mathcal{L} defined by:

$$\mathcal{L}(E, \tilde{E}) = \frac{1}{2} \|y - H(E)\|_{\mathcal{O}}^2 + \left\langle \tilde{E}, \frac{\partial E}{\partial t} + 2\nu k^2 E - T(E) \right\rangle_{\mathcal{M}} \quad (1)$$

The operator H in equation (1) is the observation operator from model space \mathcal{M} to observation space \mathcal{O} and allows for the comparison between observations y and solution $E(k, t)$. The spectrum $\tilde{E}(k, t)$ is the Lagrange multiplier for the constraint on the dynamics of $E(k, t)$. The nonlinear transfer term $T(E, k, t)$ in the governing equation for $E(k, t)$ is closed by the EDQNM approximation. Writing the necessary conditions for (E, \tilde{E}) to be a minimizer of \mathcal{L} and setting:

$$\begin{aligned} \frac{\partial E}{\partial t}(k, t) + 2\nu k^2 E(k, t) - T(E, k, t) &= 0 & (2) \\ -\frac{\partial \tilde{E}}{\partial t}(k, t) + 2\nu k^2 \tilde{E}(k, t) - \tilde{T}|_E(\tilde{E}, k, t) &= \tilde{H}|_E(y - H(E), k, t) & (3) \\ \tilde{E}(k, T_f) &= 0 & (4) \end{aligned}$$

lead to the gradient of the Lagrangian \mathcal{L} with respect to the initial condition $E^0(k) = E(k, 0)$:

$$\frac{\partial \mathcal{L}}{\partial E^0}(E, \tilde{E}, k) = -\tilde{E}(k, 0) \quad (5)$$

The operators $\tilde{T}|_E$ and $\tilde{H}|_E$ in (3) correspond to the adjoint operators of the gradients of the energy transfer term T and of the observation operator H . The above equations allow to design the following iterative optimization procedure for the reconstruction of the initial condition of the reference decay with associated observations y . We start the algorithm with a first guess for the initial energy spectrum $E^0(k)$. At the i th iteration, Lin's equation (2) is solved from $t = 0$ to $t = T_f$, where T_f is the finite duration of the decay under consideration. The solution $E(k, t)$ so obtained is used to solve backward the adjoint problem (3)-(4) from $t = T_f$ to $t = 0$. The gradient of the Lagrangian with respect to the initial energy spectrum can then be computed from equation (5). A descent method is used to update the estimated initial condition, and we can continue to next iteration. The quasi-Newton BFGS method is chosen to compute the descent method and a step length is determined by the use of bicomplex numbers. The optimization procedure is stopped after achieving a substantial reduction by six orders of magnitude in the value of the Lagrangian \mathcal{L} .

REALIZABILITY, TYPES OF OBSERVATIONS

In order to ensure the realizability condition for the energy spectrum ($E(k, t) \geq 0 \forall k, t$) during the data assimilation procedure, a functional form is prescribed for the initial energy spectrum. Two functional forms are considered for this study. The first one is the proposal by Meyers & Meneveau (2008) which accounts for all known features of the energy

spectrum. It can be written as follows:

$$E^0(k) = \begin{cases} Bk^{\sigma_1} & k < k_{L_1} \\ Ck^{-5/3}(k/k_{L_2})^{-\beta} f_L(k/k_{L_2}) f_\eta(k/k_\eta) & k \geq k_{L_1} \end{cases} \quad (6)$$

$$f_L(x) = \left(\frac{x}{[x^p + \alpha_5]^{1/p}} \right)^{5/3 + \beta + \sigma_2} \quad (7)$$

$$f_\eta(x) = \exp(-\alpha_1 x) \left[1 + \frac{\alpha_2 (x/\alpha_4)^{\alpha_3}}{1 + (x/\alpha_4)^{\alpha_3}} \right] \quad (8)$$

Equation (6) allows to distinguish the very large scales ($k < k_{L_1}$), which are characterized by the slope σ_1 , from the large scales close to the peak of the initial energy spectrum $E^0(k)$, which are characterized by the slope σ_2 . The separation between large and very large scales is fixed at $k_{L_1}/k_{L_2} = 10^{-3}$, this value ensures at least one decade between the wavenumber k_{L_1} and the final position of the peak of the energy spectrum at $t = T_f$. Both k_{L_2} and α_5 govern the position of the peak of the spectrum, and the parameter p prescribes its shape. β is the intermittency correction. k_η sets the position of the Kolmogorov scale, while the parameters $\alpha_1 - \alpha_4$ govern the shape of the spectrum at small scales and the bottleneck correction. The constants B and C are used for normalization and preserve the continuity of the energy spectrum at $k = k_{L_1}$. The advantage of this functional form is that a small number of parameters (11) is used for the description of the initial energy spectrum, which may facilitate optimization. The data assimilation procedure will allow to identify the parameters of (6)-(8) that determine the decay. However, this functional form precludes a detailed scale-by-scale analysis, and we also consider a second functional form which is written as:

$$E^0(k) = B(k)k^{s(k)} \quad (9)$$

where $s(k)$ is the local slope of the initial energy spectrum and forms the control vector in the optimization procedure (instead of $E^0(k)$), while $B(k)$ ensures the continuity of the spectrum.

In this study, we use several types of observations of the reference decay. A first possibility is to observe the kinetic energy spectrum $E(k, t)$ itself at different times during the decay. We also consider the observations of statistical integral quantities with physical meaning such as the kinetic energy K , the integral scale L and the dissipation rate ε . Finally, we use the observation of the power-law exponent n_K driving the decay of K . Various assimilation window sizes T_f and frequencies of observations are considered.

DATA ASSIMILATION EXPERIMENTS BASED ON THE MEYERS-MENEVEAU MODEL

We first consider data assimilation experiments based on the Meyers-Meneveau spectrum model defined by (6)-(8). The size of the assimilation window T_f is fixed at 10^4 initial eddy turn-over times τ_0 . The reference decay corresponds to a Saffman turbulence ($\sigma_1 = \sigma_2 = 2$ in (6)-(7)) at high Reynolds number (the initial value of the Taylor microscale-based Reynolds number is $Re_\lambda = 800$). Ten observations of the reference decay are performed between $t = 10^3 \tau_0$ and $t = T_f$, which ensures to witness a fully developed isotropic turbulence. The estimated initial energy

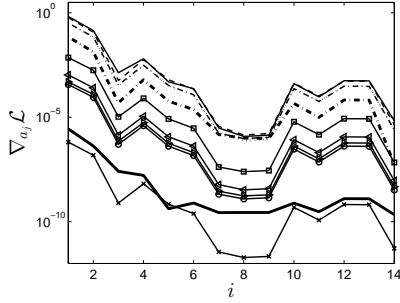


Figure 1: Derivatives of the Lagrangian \mathcal{L} with respect to the different parameters in (6) (σ_1 , σ_2 , β , p , k_{L_2} , α_1 , α_2 , α_3 , α_4 , α_5 and k_η) versus the number of iterations of the optimization procedure. The kinetic energy K is observed.

spectrum used to initialize the optimization procedure is obtained by perturbing by $\pm 10\%$ the values of the parameters of (6)-(8) chosen for the reference initial energy spectrum. Several data assimilation experiments are performed with different types of observations. Figure 1 illustrates results in the case where the kinetic energy K is observed. The partial derivatives of the Lagrangian \mathcal{L} with respect to the different parameters in (6)-(8) and their evolutions according to the iteration of the optimization procedure are reported. We notice that the value of these derivatives at the beginning of the data assimilation procedure varies widely depending on the parameter considered. The leading parameters are the slope at large scales close to the peak of the energy spectrum σ_2 , and the parameters k_{L_2} , α_5 and β that determine the initial position of the peak of the energy spectrum and the intermittency correction. The parameter p plays an intermediate role, while the influence of α_1 - α_4 that parametrize the shape of the energy spectrum at small scales seems marginal. It also appears that the sensitivity of the Lagrangian with respect to the slope at the largest scales σ_1 is negligible. These results indicate that, contrary to the large scales close to the peak of the energy spectrum, the largest scales do not play a significant role in the decay. A reduction by 5 orders of magnitude in the values of the derivatives of the Lagrangian with respect to the parameters of (6)-(8) is achieved, which means that the data assimilation procedure has converged. Figure 2 reports the evolution of the relative errors on the slopes σ_1 and σ_2 , defined as the relative differences between the true values of these slopes and the estimated ones, for different data assimilation experiments associated to different types of observations: the kinetic energy spectrum $E(k, t)$, the kinetic energy K , the integral scale L , the dissipation rate ε , or a combination of these statistical integral quantities. No error reduction is achieved for the slope σ_1 , even when quantities which are *a priori* the most sensitive to large scales such as the energy spectrum itself or the integral scale are observed. In contrast, the true value of the slope σ_2 is recovered with good accuracy (relative error about 10^{-3} at the end of the data assimilation procedure) in all cases. This confirms that the value of the slope σ_1 at the largest scales has no significant influence on the decay. The gradient of the Lagrangian \mathcal{L} with respect to the initial energy spectrum for the different data assimilation experiments is given in figure 3. From the comparison between figures 3(a) and 3(b), it appears that the maximum of the

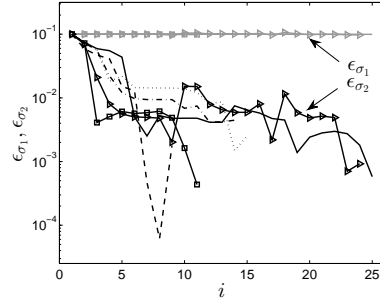


Figure 2: Relative errors on the slope at the largest scales σ_1 (grey lines) and on the slope at the large scales close to the peak of the initial energy spectrum σ_2 (black lines) versus the number of iterations of the optimization procedure. The six types of lines (besides color) correspond to different types of observations: $E(k)$, K , L , ε , $K+L$ and $K+L+\varepsilon$. The kinetic energy K is observed.

sensitivity of the Lagrangian is reached at a wavenumber close to the position of the peak of the energy spectrum at the end of the assimilation window. This gradient vanishes at small scales in roughly the same way for the different types of observations, but exhibits different shapes at large scales. These shapes can be easily recovered by considering the discrete expressions of the observed quantities in terms of the energy spectrum. In the case where the observation of the reference decay is a scalar, the slope at large scales of the gradient of the Lagrangian with respect to the initial energy spectrum does not depend either on the characteristics of the true initial energy spectrum or on those of the estimated spectrum. For example, when the kinetic energy K is observed, $\frac{\partial \mathcal{L}}{\partial k} \propto k$ at large scales whatever the features of the true and estimated energy spectra, meaning that only large scales close to the peak of the energy spectrum lead the decay.

DATA ASSIMILATION EXPERIMENTS BASED ON A SCALE-BY-SCALE DESCRIPTION

The functional form (9) is now prescribed for the initial energy spectrum. The control vector is formed by the local slope $s(k)$ of the initial energy spectrum and its dimension is equal to the number of resolved modes ($= 165$). The true initial energy spectrum, the size of the assimilation window, the number of observations and their distribution in time are the same than for the data assimilation experiments of previous section. In order to confirm the robustness of the results established in the present work, three types of estimated initial energy spectra are used as first guesses for the optimization procedure for the reconstruction of the reference initial energy spectrum. The first one (type A) corresponds to a constant perturbation of -25% of the true value of the slope at large scales. The inertial and the dissipative ranges are respectively defined by a constant slope. For the second type of estimated initial energy spectra (type B), a random slope is assigned for the initial energy spectrum each half-decade. The slopes at large scales are picked between 1 and 4. The third type (type C) corresponds to the assignment of a random local slope for each of the energy modes. We consider three data assimilation experiments which use the different estimated initial energy

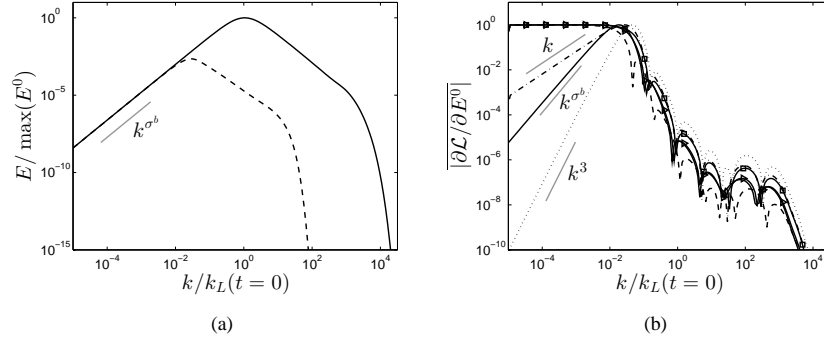


Figure 3: (a) Estimated energy spectra at $t = 0$ (full lines) and at $t = T_f = 10^4 \tau_0$ (dashed lines) at the first iteration of the optimization procedure; (b) gradient with respect to the initial energy spectrum E^0 of the Lagrangian \mathcal{L} for different types of observations: — $E(k)$, \cdots K , - - - L , - \cdot - \cdot ε , $\text{--}\blacktriangleright$ $K + L$ and $\text{--}\blacksquare$ $K + L + \varepsilon$.

spectra discussed above, and where the exponent n_K driving the decay of the turbulent kinetic energy as $K(t) \propto t^{n_K}$ is observed. The interest of using the observation of the exponent n_K is that n_K furnishes a purely dynamical information about the decay that can be easily compared with most experimental data. Results concerning these three numerical assimilation experiments are reported in figure (4). Figure 4(a) illustrates the evolution of the value of the cost function $J(E) = \frac{1}{2} \|y - H(E)\|_{\mathcal{D}}^2$ with respect to the iteration of the optimization procedure. The three experiments have achieved a reduction by six orders of magnitude in the value of the cost function. Figure 4(b) reports the difference between the values of the local slope of the estimated initial energy spectrum at the end and at the beginning of the optimization procedure. A non-zero value for this difference means that the corresponding zone of the estimated spectrum has been modified by the assimilation procedure. It appears that, in all cases, only a narrow region of the estimated spectrum has been corrected by the optimization procedure, which is located roughly between the positions of the peak of the energy spectrum at the beginning and at the end of the assimilation window. The estimated spectrum has not been modified at scales ten times bigger than the integral scale at the end of the assimilation window, whereas the shape of the estimated spectrum at the largest scales significantly differs from that of the reference initial energy spectrum (see figures 4(d)-4(f)). The gradient of the Lagrangian \mathcal{L} with respect to the initial energy spectrum is reported in figure 4(c) for the different assimilation experiments. In all cases it appears that $\frac{\partial \mathcal{L}}{\partial E^0} \propto k$ at large scales as in the case where the kinetic energy is observed. This result can be recovered analytically from the Gâteaux derivative of the expression of the exponent n_K obtained from the evolution equation of the kinetic energy K in the case of HIT. This result is independent of the features of the considered energy spectrum. As for the assimilation experiments of previous section with other types of observations, the maximum of sensitivity of the Lagrangian is located at the integral scale of the energy spectrum at the end of the assimilation window (figure 3 is scaled with the initial position of the integral scale at wavenumber $k = k_L(t = 0)$ whereas figure 4 is scaled with the final position of the integral scale $k_L(t = T_f)$). The reference, estimated and retrieved at the end of the optimization procedure initial spectra are illustrated in figures 4(d)-4(f) for the three experiments. As mentioned above, although the optimization procedure has converged in all cases, the

true shape of the estimated spectrum at the largest scales has not been recovered. Only the slope of the estimated spectrum has been corrected between the positions of the peak of the energy spectrum at the beginning at the end of the assimilation window (see e.g. figure 4(h)). This is consistent with the fact that observing the decay exponent only, one has no control of the absolute value of the kinetic energy. It also shows that, if the kinetic energy is high enough to sustain high-Reynolds number evolution, without transition to low-Reynolds number regime (which exhibits different decay exponent values), only the shape of the large scale energy spectrum matters.

CONCLUSION

This study was devoted to the analysis of grid turbulence decay, with the purpose of identifying scales and related features of the energy spectrum that govern the decay regime. To this end, an optimal-control-based data assimilation technique was employed. The present results show that the decay of grid turbulence is not governed by the asymptotic large scale behavior of the energy spectrum $E(k \rightarrow 0, t = 0)$. This conclusion is robust, since it is observed in all cases considered, that mix both full energy spectrum and integral observations and both Meyers-Meneveau parametric spectrum model and local scale-by-scale initial spectrum model. Further results can be found in Mons *et al.* (2014). The decay regime over finite time is governed by large scales ranging approximately from the initial integral scale to the final integral scale, a vanishing sensitivity being observed for large scales located within one decade outside these bounds. The most important feature is the shape of the spectrum in this range. If a slope can be identified, then Comte-Bellot-Corrsin's formula yield an accurate prediction of the decay regime. According to present observations, large scales should be understood as scales slightly larger than the integral scale $L(t)$ such that $kL(t) = O(1)$. This is coherent with previous studies dealing with evolution of initially non-self-similar energy spectra (Meldi & Sagaut, 2012). Another point here is that in wind tunnel grid turbulence the largest scales are anisotropic and non-homogeneous due to wall effects, but this breakdown of homogeneity at very large scales is not observed to significantly corrupt the nearly isotropic behavior reported by many researchers. This is coherent with the present conclusions.

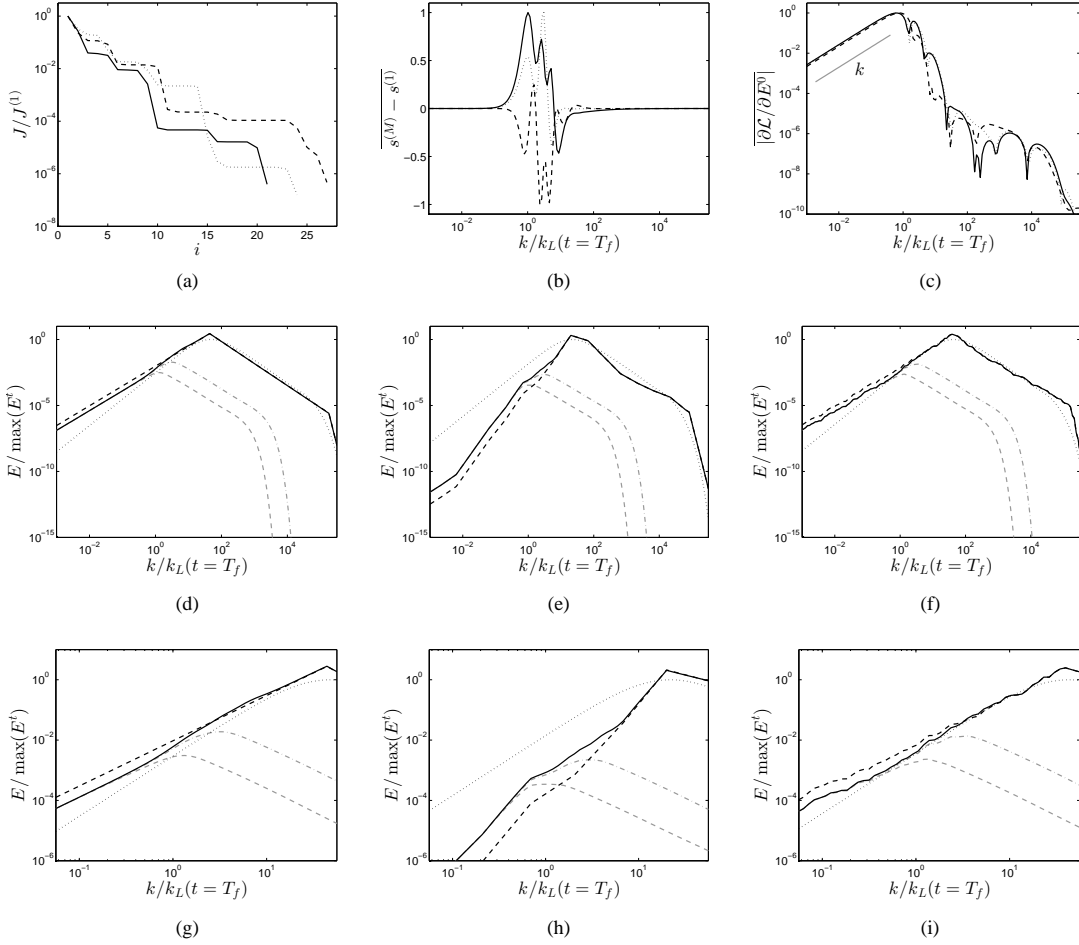


Figure 4: First row: (a) Value of the cost function J normalized by its initial value, (b) difference between the local slope of the initial energy spectrum obtained at the end of the optimization procedure (iteration (M)) and that of the spectrum at the first iteration (i.e. the estimated spectrum), and (c) gradient with respect to the initial energy spectrum E^0 of the Lagrangian \mathcal{L} (at the first iteration of the optimization procedure). The three types of lines correspond to different estimated initial spectra: — type A, - - - type B, type C. Second row: true (black dotted line), estimated (black dashed line) and retrieved at the end of the optimization procedure (black full line) initial energy spectra when the estimated initial energy spectrum is of type A (d), B (e) and C (f). The energy spectra at $t = 10^3 \tau_0$ (dash-dotted grey lines) and at $t = T_f = 10^4 \tau_0$ (dashed grey lines) are also reported in the figures. A zoom of Figures (d)-(f) in the vicinity of the peak of the energy spectrum at $t = T_f$ is reported in Figures (g)-(i). The decay exponent n_K is observed.

REFERENCES

- Comte-Bellot, G. & Corrsin, S. 1966 The use of a contraction to improve the isotropy of grid-generated turbulence. *Journal of Fluid Mechanics* **25**, 657 – 682.
- Le Dimet, F. X. & Talagrand, O. 1986 Variational algorithms for analysis and assimilation of meteorological observations: theoretical aspects. *Tellus* **38A**, 97–110.
- Meldi, M. & Sagaut, P. 2012 On non-self-similar regimes in homogeneous isotropic turbulence decay. *Journal of Fluid Mechanics* **711**, 364–393.
- Meyers, J. & Meneveau, C. 2008 A functional form of the energy spectrum parametrizing bottleneck and intermittency effects. *Physics of Fluids* **20**, 065109.
- Mons, V., Chassaing, J.-C., Gomez, T. & Sagaut, P. 2014 Is grid turbulence decay governed by asymptotic behavior of large scales ? A Data Assimilation study. *Physics of Fluids* **26**, 115105.
- Orszag, S. A. 1970 Analytical theories of turbulence. *Journal of Fluid Mechanics* **41**, 363 – 386.
- Sagaut, P. & Cambon, C. 2008 *Homogenous Turbulence Dynamics*. Cambridge University Press.